Quasi-elastic scattering of electrons at large momentum transfer

M. Vos†, **G. Cooper**‡ **and C.A. Chatzidimitriou-Dreismann**§

† Atomic and Molecular Physics Laboratories, Research School of Physical Sciences and Engineering, Australian National University, Canberra, ACT, 0200, Australia

‡ Department of Chemistry, McMaster University, Hamilton, Ontario, L8S 4M1, Canada

§ Institute of Chemistry, Stranski Laboratory, Technical University Berlin, Strasse des 17. Juni 112, D-10623 Berlin, Germany

Abstract. Precision measurements of the energy of keV electrons scattered 'elastically' over large angles from solid films or gas-phase molecules show that these electrons have lost some energy. In particular scattering from a system that contains hydrogen and carbon reveals two well-separated elastic peaks. The amount of energy lost in the deflection of the electron depends not only on the mass of the nucleus the electron scattered from, but also on the momentum of this nucleus. We make an estimate of the cross section for these elastic scattering processes. These cross sections do not reproduce the observed intensities very well, in particular the observed hydrogen intensity is for the solid film experiment smaller than expected. With increasing energy loss the time-scale of the collision process decreases. The decrease of the hydrogen cross section is possibly due to quantum correlation effects of the proton at the short timescale of the collision.

1. Introduction

It is well known that the region probed in a scattering experiment depends on the momentum transfer $\boldsymbol{q}$. The intensities originating from sources separated by $r >> 1/q$ add incoherently. If $r \leq 1/q$ one has to add the intensity coherently, leading to phenomena such as diffraction. At very large momentum transfer there is no structure left in the target, at a scale of $1/q$ and we have binary collisions from either a nucleus or an electron in the system. Thus in an electron scattering experiment at very large momentum transfer, one scatters from either a single electron or a single nucleus (i.e. a binary collision). If one scatters from an electron a significant fraction of the kinetic energy is transferred and these scattering events are studied in, e.g., $(e, 2e)$ experiments. Here we restrict ourselves to electrons scattered from nuclei.

If one assumes that the target (mass m_t) is initially at rest (momentum $p_t = 0$), then a momentum transfer of an amount q implies that after the collision $p_t = q$ and hence it has an energy $q^2/2m_t$. This energy transfer should be reflected in a decrease in energy of the elastically scattered electron. The question is, which mass m_t should we consider: the mass of the whole solid or molecule or that of an individual nucleus. Experimentally it was shown by Boersch *et al* [1] as early as 1967 that at large momentum transfer the energy loss of the scattered electron is consistent with scattering from an individual nucleus.

If the target nucleus (mass m) has initially a momentum $\boldsymbol{p}_0$, then the energy transfer ω to the target is

$$\omega = \frac{(\boldsymbol{p}_o + \boldsymbol{q})^2}{2m} - \frac{p_o^2}{2m} = \frac{q^2}{2m} + \frac{\boldsymbol{p}_0 \cdot \boldsymbol{q}}{m} \tag{1}$$

Thus if the mass of the scatterer is known the measurement resolves a component of the momentum of the nucleus in a similar way as Compton scattering of an X-ray from an electron resolves a component of the electron momentum.

In spite of the work of Boersch *et al* it was generally believed that the energy transfer of an electron scattered from a nucleus was too small to be measured. It was realised that the momentum distribution of nuclei in materials (in particular the zero-point motion of the nucleus in its ground state) was determined by the strength of the bond, and hence was of fundamental interest. A technique was developed using neutrons to measure these momentum distributions, usually referred to as Neutron Compton Scattering (NCS) [2]. The theory behind these neutron scattering experiments is well established [2, 3, 4].

In the next section we present electron scattering data for both thin films and gas phase targets. The signal of electrons scattered from carbon and hydrogen atoms is well separated, and the effect of target motion is resolved. There appear to be problems reconciling the measured hydrogen intensity with the theoretically expected one for the thin film targets. We will explain that in the high-energy limit the electron scattering experiments are described by the same theory as the NCS experiments and compare our data with NCS experiments. Target properties obtained by neutron are in good agreement with those obtained from electron scattering experiments. For both probes a smaller hydrogen signal than expected was found. We will stress that these experiments probe the target on a very short time scale. It is argued that the shortfall in proton-derived intensity could be due to quantum correlations in the proton wave function at these short time scales.

2. Experimental Results

The electron scattering results for the polyethylene (PE) film were obtained using the ANU electron momentum spectrometer [5]. Thin, free-standing, samples ($\simeq 10$ nm thick) were obtained using a method derived from the procedure described by Cranfill [6] and the one described by Godovsky and Magonov [7]. The polyethylene was dissolved in xylene at 100 °C (0.1% by weight). A microscope slide was partly submerged in this solution, and after it was thermally equilibrated, it was slowly (0.5 - 1 cm per minute) pulled out of the hot solution, leaving the slide coated with a thin PE film. After cooling down and drying the microscope slide was slowly submerged in distilled water with a 10-20° angle between the microscope slide and water surface. The PE film separates from the microscope slide and floats on the water surface. This film was then transferred to the sample holder, covering many holes.
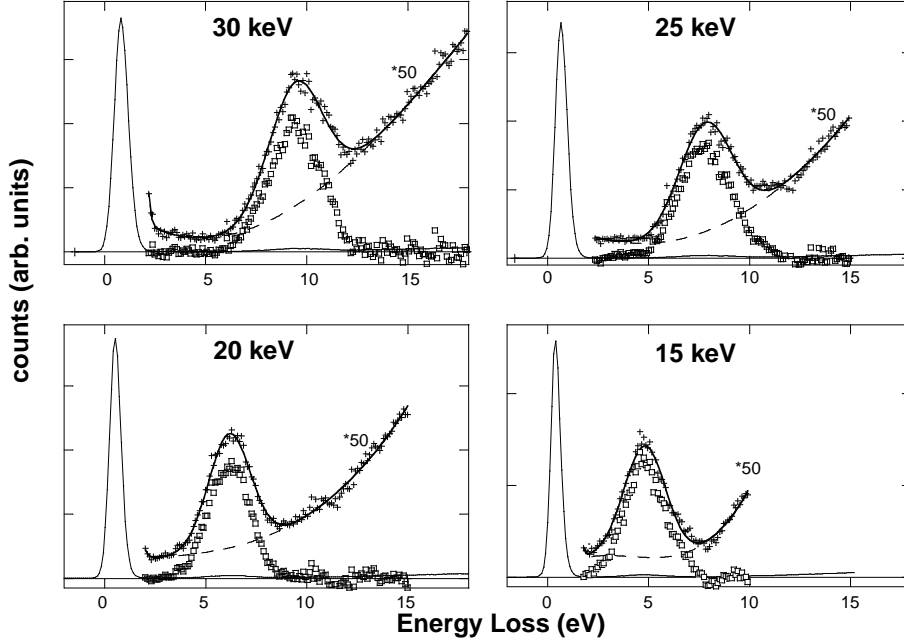
Figure 1. Energy loss spectra of polyethylene. Spectra are obtained for incoming electron energies as indicated. Besides the major elastic peak (attributed to electrons scattered from carbon) there is a second, small peak (shown as a + on the 50 times expanded scale) at larger energy loss values(attributed to electrons scattered from hydrogen). The separation of this peak relative to the main peak is proportional to the incoming energy. The background is shown as a dashed line, the fit as a full line and the background subtracted hydrogen peak as open squares.

The energy loss spectra, obtained for a scattering angle of $45°$ and electron energies between 15 and 30 keV, are shown in Fig. 1. As the precise zero energy-loss position of the spectrometer is difficult to determine we aligned the energy scale in such a way that the main peak position corresponds to the energy loss expected for scattering from a single carbon atom. The spectra all show a smaller peak at larger loss values superimposed on a background. The background is due to electrons that have scattered elastically from a carbon atom *and* have created an electronic excitation in the film. The shape of the background should resemble the energy loss spectra as measured in the forward direction. In particular this shape should not change with the energy of the probing electron. As the smaller peak is at an energy loss value proportional to the incoming energy, it can not be due to an elastic deflection plus electronic excitation. Indeed its position is what one would expect for quasi-elastic scattering from a

target	Θ	E_0	$|q|$	ΔE_{obs}	ΔE_{calc}	Γ_{obs}	Γ_{calc}	$I_H:I_C$	$I_H:I_C$
	deg.	(keV)	(a.u.)	(eV)	(eV)	(eV)	(eV)	obs.	calc.
PE	45	30	35.9	8.6	8.75	3.1	3.2	1:24.9	1:18
PE	45	25	32.9	7.1	7.35	3.1	2.9	1:24.4	1:18
PE	45	20	29.2	5.6	5.8	2.5	2.6	1:29	1:18
PE	45	15	25.6	4.4	4.45	2.4	2.3	1:25.1	1:18
CH_4	100	2.0	18.6	2.15	2.4	1.7	1.7	1:10.1	1:9

Table 1. A summary of the measured and calculated separation of hydrogen from the main peak, full width half maximum Γ of the hydrogen peak and the intensity ratio of the hydrogen peak I_H and main peak I_C
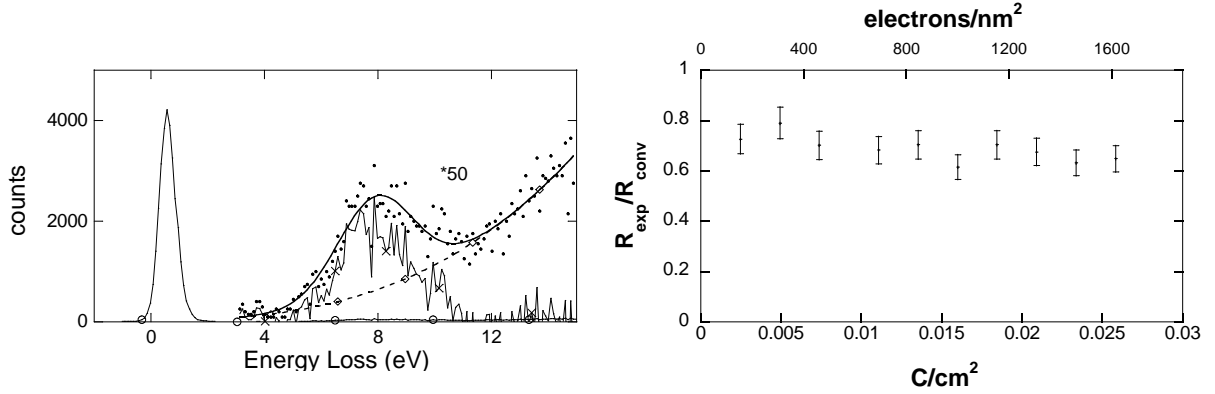
3

Figure 2. The left panel shows the quality of a polyethylene spectrum obtained in two minutes and the decomposition of the signal (dots) in background (dotted line) and proton signal (full line, magnified part. A series of two minute measurements was performed. The dependence of the R_{exp}/R_{conv} (measured hydrogen peak area relative to the expected peak area) as a function of accumulated beam charge is displayed in the right panel. The R_{exp}/R_{conv} ratio decreases slowly with dose. However this decrease is much too slow to explain the observed anomaly.

single proton. The spectra were fitted by two Gaussians and a polynomial background. The results of this fitting procedure is summarised in table 1.

The width of the proton-derived elastic peak is clearly much larger than the width of the carbon peak (and even the carbon peak is wider than the experimental resolution [8]). This extra width is due to Doppler broadening induced by the motion of the nucleus (see Eq. 1). Thus we have here a clear signature of the proton momentum distribution. For a proton in an isotropic, harmonic potential the momentum distribution is Gaussian, and the observed width is conveniently expressed in terms of the recoil energy and the mean kinetic energy of the atoms $\overline{E_k}$. The standard deviation σ of the observed Gaussian is given by [9]:

$$\sigma = \sqrt{\frac{4}{3}\overline{E_k}E_r},\tag{2}$$

with E_r the mean recoil energy. As a first approximation all C-H bonds will be rather similar. If we take ethane (C_2H_6) as an example it has a calculated zero-point energy of 2 eV per molecule [10]. Half of this will be kinetic energy. Most of the kinetic energy will be in the lighter atoms, so we expect around 0.15 eV kinetic energy per proton. For hydrogen in hydrogenated amorphous carbon Mayers et al measure 146 meV using NCS [11], and they estimate on theoretical grounds energies between 156 and 183 meV for hydrogen in C-H bonds. Using Eq. 2 and a mean proton kinetic energy of 0.15 eV one obtains the estimate of the full-width half maximum given in table 1. The agreement between the observed and calculated values of the carbon-proton peak separation and the proton peak width is quite satisfactory.

For now we used a crude model for the cross section, assuming simply that at these momentum transfers the cross section is equal to the Rutherford cross section. From the known composition of polyethylene $(-CH_2-)_n$ and these cross sections we can make an estimate of the ratio of the carbon-hydrogen peak areas. We use a polynomial fit of the background as indicated with a dashed line in Fig. 1. Using the Rutherford cross section for electrons and the known composition of the target we can calculate the expected ratio of the hydrogen to carbon peak. We call this ratio R_{conv}. The observed ratio R_{obs} of the hydrogen peak relative to the
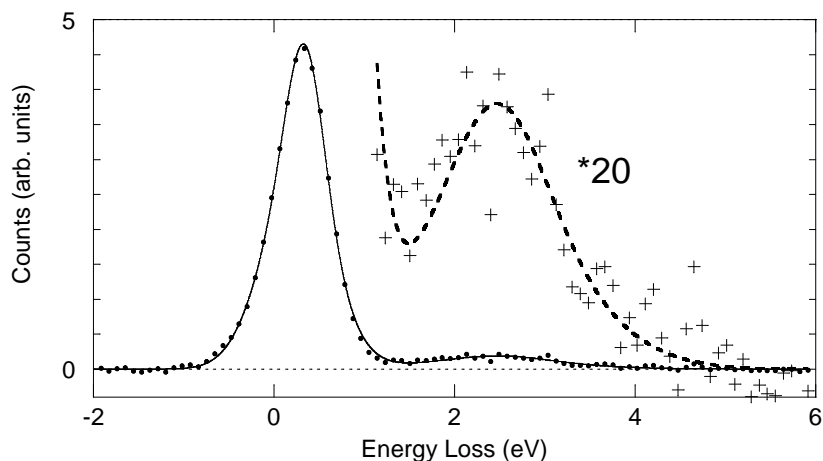
4

Figure 3. The spectrum of 2 keV electrons scattered over 100° from methane. Again two peaks are visible, consistent with electrons scattering from either C or H. The measurement is fitted with two Gaussians and a constant background (subtracted in the figure), as indicated by the full line (dashed line in the 20* magnification).

carbon peak is smaller than the calculated ratio R_{conv}. It appears as if some (about 25 %) of the protons are invisible.

In electron scattering experiments one has to be careful as the electron beam may cause a change in composition of the film. The impinging electrons can break a chemical bond and a hydrogen atom may subsequently desorb, leaving a carbon-rich film behind. In order to test if radiation damage is the cause of the smaller than expected hydrogen peak area, we studied the signal as a function of electron dose. By keeping the carbon-hydrogen peak separation fixed at the established value in the fitting routine, as well as the hydrogen and carbon peak width, we could obtain reasonably accurate peak areas for spectra taken with a low dose of electrons. We found a small dependency of R_{obs}/R_{conv} on electron exposure (see Fig.2), however this dependency was too weak to explain the observed discrepancy.

These results are intriguing. Are similar measurements possible using gas-phase targets? This would truly eliminate the problem of radiation damage, as in these effusion experiments the target is continuously replenished. Also the target density will generally be low enough that multiple scattering effects are absent, i.e. we do not have to subtract a poorly known background.

For this purpose we made preliminary measurements using the McVAHRES spectrometer at McMaster University[12]. The maximum incoming energy (2 keV) and scattering angle (100°) attainable in this spectrometer were chosen. The signal was weak, and a constant background had to be subtracted. The results are shown in Fig. 3. Again the main peak was aligned with the expected energy loss for electrons scattered from carbon under these conditions (0.2 eV). There is indeed again a broader satellite now at the energy loss of just over 2 eV, but now there is no background increasing with energy loss. The spectra could be fitted using two Gaussians and a constant background term. The fitting results are summarised in table 1 as well. The peak width and separation is in good agreement with the calculated one. Preliminary indications are that the carbon to hydrogen peak area ratio is closer to the theoretical expected one than in the polyethylene case.
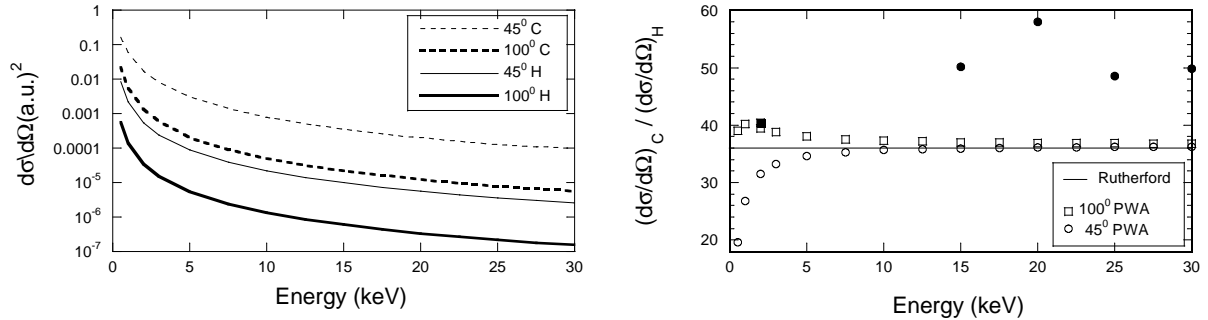
5

Figure 4. The differential cross section, as calculated in using partial waves [13] as a function of energy at 45° and 100° for carbon and hydrogen atoms (left panel) as well as their ratio (right panel). The calculated cross section ratio (open symbols) approaches with increasing energy the value of $(Z_1/Z_2)^2$ (presented by the full line) as predicted by the Rutherford cross section. Experimental cross section ratios are plotted as well, represented by filled symbols

3. Theory

In the previous section we assumed that the cross section for electron scattering was just proportional to Z^2, and the width was proportional to the momentum component of the proton along $\boldsymbol{k}$. This is a simple picture, relying completely on classical physics. It is just like Rutherford backscattering, using electrons, rather than ions as the probing particles.

Nowadays elastic scattering of electrons from atoms is usually treated as potential scattering. The potential is due to the charge of the nucleus, presented as a point charge, and the charge density associated with the electron wave function. At low momentum transfer the screening of the target electrons is crucial as it cancels the long-range tail of the nuclear Coulomb potential. At high momentum transfer the scattering occurs in a much smaller region around the nucleus and screening should become less important. Within potential scattering theory there is no energy transfer from the electron to the target and thus we can not distinguish electrons scattered from different nuclei. Hence we can not completely describe these measurements by just replacing the spherically symmetric potential of an atom by a molecular potential of lower symmetry.

The scattering at large momentum transfer happens close to a nucleus, where the electronic structure is similar in the molecule compared to the atom. We assume thus that for large momentum transfers scattering from an atom in a molecule, is the same as scattering from a single atom. This can be treated by standard potential scattering theory. If the momentum transfer is so large that in a volume with radius $1/q$ around the nucleus the total electron charge density is small the approximation of the potential by a Coulomb potential should become reasonable. Hence the differential cross section should approach the Rutherford value. In order to investigate this further we calculated the differential elastic cross section for isolated atoms using the partial wave formalism. We used the code written by Salvat and Mayol [13]. Exchange and relativistic effects are included in this code but polarisation effects are not considered. In Fig. 4 we plot the differential cross section as a function of energies for scattering angles of 100 and 45 degrees, as well as the ratio of the carbon and hydrogen cross section. This ratio approaches at higher energy the ratio predicted by the Coulomb cross section within a few percent.

Of course the charge distribution in molecules is modified compared to the free atom.

6

The main influence on the cross section at high momentum transfer will be due to the carbon 1s electrons, as these electrons are most effective in screening. These electrons are not expected to change significantly due to the chemical bond. Thus we conclude that under the present conditions errors introduced by assuming scattering from a Coulomb field to be of the order of a few percent, an order of magnitude smaller than the observed discrepancies.

In the previous section we use potential scattering theory for obtaining the cross section, and we derive the energy loss of the scattering event from a classical argument based on the finite mass and momentum of the target. For weakly interacting probes such as neutrons we can describe the scattering experiments in the first Born approximation and a single quantum theory has been developed that describes the observed intensity and energy loss distribution. Here we quote some of the results of this theory, a full description can be found in the neutron literature [2, 3, 4]. In the first Born approximation it can be shown that

$$\frac{d^2\sigma}{d\Omega d\varepsilon} = AS(\boldsymbol{q}, \omega) \tag{3}$$

$$A = \frac{m^2}{4\pi^2} \frac{k_1}{k_0} W(q)$$

$$W(q) = \left(\int \exp(i\boldsymbol{q} \cdot \boldsymbol{r}) V(\boldsymbol{r}) d\boldsymbol{r} \right)^2.$$

Here m is the mass of the projectile, $\boldsymbol{k}_0$ and $\boldsymbol{k}_1$ the momentum of the scattered particle before and after the collision, and $V(\boldsymbol{r})$ the particle-target interaction. $S(\boldsymbol{q}, \omega)$ is the dynamical structure factor, a target property.

$S(\boldsymbol{q}, \omega)$ is the Fourier transform in space and time of the pair distribution function $G(\boldsymbol{r}, t)$

$$S(\boldsymbol{q}, \omega) = \frac{N}{2\pi} \int e^{i(\boldsymbol{q} \cdot \boldsymbol{r} - \omega t)} G(\boldsymbol{r}, t) d\boldsymbol{r} dt \tag{4}$$

with N the particle density [3]. $G(\boldsymbol{r}, t)$ is generally a complex function, but is real for classical particles. Then it is simply the density distribution at $\boldsymbol{r}$ and time t as seen from the point $r = 0$ where a particle passed at $t = 0$. $G(\boldsymbol{r}, 0)$ is the (real) pair distribution function and is probed in truly elastic scattering (e.g. diffraction).

For large $\boldsymbol{q}$ and $\boldsymbol{r}$ (corresponding to different atom positions) the integrant in Eq. 4 is rapidly fluctuating and will not contribute much to the integral. Thus $G(\boldsymbol{r}, t)$ is probed over a region $r \simeq 1/q$ and hence at large q values we have essentially binary collisions with single atoms. (This is in the neutron literature referred to as the incoherent approximation.) The characteristic width of $S(\boldsymbol{q}, \omega)$ is proportional to $\overline{p_q} q / m$ with $\overline{p_q}$ the root mean square momentum component of the target atom along $\boldsymbol{q}$ (see Eq. 1). There is no structure in $S(\boldsymbol{q}, \omega)$ at a smaller energy scale. That means that the longest characteristic time scale of interest in the Fourier transform is $t = m/(\overline{p_q} q)$ [2]. This time is considered to be the scattering time τ. It decreases with increasing values of q. For the current experimental conditions $\tau \leq 10^{-15}$ sec.

In the previous paragraphs (e.g. in the derivation of Eq. 1) we assume that we can treat the collision between an electron (neutron) with a nucleus as a collision between two free particles. This is usually referred to as the impulse approximation. If the impulse approximation applies $S(\boldsymbol{q}, \omega)$ simplifies to [4]:

$$S(\boldsymbol{q}, \omega) = \delta(\omega - \frac{q^2}{2m} - \frac{\boldsymbol{p}_0 \cdot \boldsymbol{q}}{m}) \tag{5}$$

and hence we can measure a projection of the momentum distribution of the nucleus.

Does this approach apply as well to the present electron scattering measurements? The validity of the Born approximation is not as easily justified for strongly interacting particles such as electrons as it is for weakly interacting neutrons. In the high-energy limit the interaction of an electron with a single atom becomes weak and Eq. 3 should become a reasonable description of the experiment. From measurements of noble gases we know that the differential elastic cross section of $\simeq 40$ keV electrons from argon is well described by the first Born approximation but the approximation breaks down for higher Z species such as xenon [14, 15]. Hence we expect the first Born approximation (and hence the factorisation of Eq. 3) to provide a reasonable description for 25 keV electrons scattering quasi-elastically from molecules composed of light elements, such as carbon, oxygen and hydrogen, but it may fail at lower energies and/or if heavier elements are involved.

The only part of Eq. 3 that depends on the probing particle is the projectile-target interaction $V(\boldsymbol{r})$ and the projectile mass m. As these quantities are known for both neutrons and electrons we can compare neutron and electron scattering experiments to test explicitly if Eq. 3 gives a consistent description of both experiment. A comparative study, using polyethylene as a target has been described extensively in [16] and we summarise the main points here.

In order to have similar momentum transfer as in our electron scattering experiment one has to scatter neutrons with energies around 20 eV. These NCS experiments were done at the Vesuvio beam line of ISIS and use a pulsed neutron beam in combination with filters with sharp absorption dips to determine the neutron energy loss by a time-of-flight technique [17]. Let us first compare the proton momentum distribution as measured by electron and neutron scattering. This is displayed in the left panel of Fig. 5. Using Eq. 1 or Eq. 5 we can calculate from the measured energy transfer distribution the proton momentum distribution. In the left panel of Fig. 5 we plot the width of the proton momentum distribution as a function of momentum transfer. The proton momentum distribution is indeed independent of the momentum transfer, and within the spread of the measurement, the same results are obtained for protons and neutrons. In the right panel of Fig. 5 we plot the R_{obs}/R_{conv} values found for both technique as a function of momentum transfer. For neutrons one can calculate the same ratio R_{obs}/R_{conv} based on the known neutron cross sections of H and C [18]. For both electrons and neutrons R_{obs}/R_{conv} is systematically less than 1 by a similar amount. For neutron scattering these effects are known from a large group of proton containing materials [19, 20, 21]. Thus also the anomalous neutron scattering cross section seems to be reproduced by the electron experiment. Similar agreement between the electron and neutron measurement was found for formvar, a different polymer [22].

In summary at high-enough incoming energy and momentum transfer we expect the results of electron scattering to be directly comparable with the neutron data. These conditions are probably well full-filled at the high energies described here (30 keV) but more questionable for the 2 keV experiment. Indeed in the comparative study of neutron and electron scattering experiments of polyethylene good agreement was found between both techniques.

In reality the nucleus is bound as it is part of a molecule. The energy transfer to the proton is of the order of the bond energy. However the impulse approximation can still be valid, even if the energy transfer is less than the bond strength [2]. One way of explaining the working of the impulse approximation under these conditions is to say that during the interaction time the nucleus moves over such a small distance that it does not feel any change in potential. The interaction time is inversely proportional to the transferred momentum. It does not relate to the 'velocity' of the scattered particles. Note that the velocity of a 25 keV
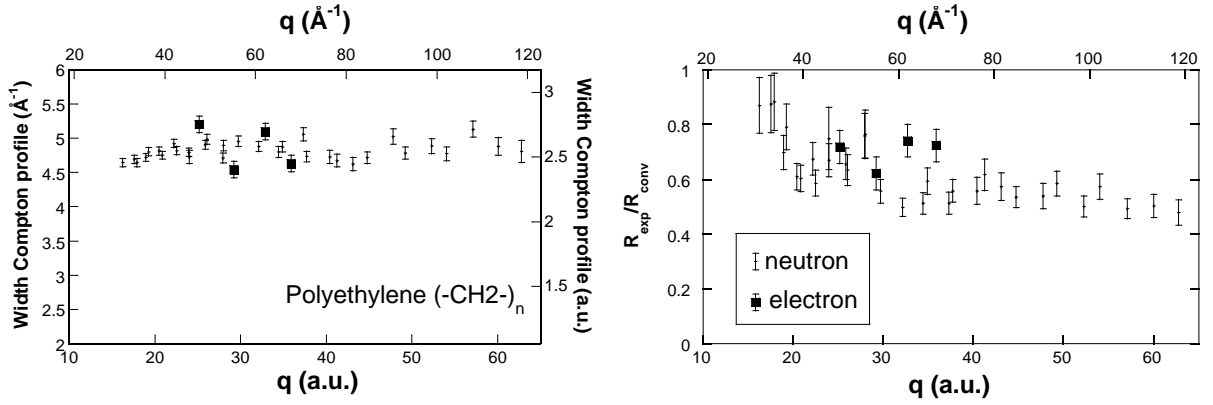
Figure 5. Results for a polyethylene film as obtained by neutrons and electrons. A comparison of the dependence of the width of the Compton profile on the momentum transfer is shown in the left panel. The observed hydrogen-to-carbon peak area ratio R_{exp} divided by the calculated ratio R_{conv}, based on the calculated cross sections, is shown in the right panel.

electron is more than 1000 times that of the velocity of a 25 eV neutron. Thus the proposition that the impulse approximation is independent of the velocity of the probing particle could be tested in a suitably-designed experiment using both electrons and neutrons.

$G(\boldsymbol{r},t)$ is a function of $\boldsymbol{r}(t)$: the Heisenberg operator $exp(itH)r(0)exp(-itH)$. Hence for $t > 0$, $G(\boldsymbol{r},t)$ becomes complex [3]. The protons and electron wave function are coupled by the Coulomb matrix elements and the system will not separate in the product of an electron wave function and a proton wave function. For large t the proton will have interacted with the environment and the phase information is lost. Due to this decoherence the proton will have lost the capability to interfere, and acts like a classical particle, i.e. $G(\boldsymbol{r},t)$ becomes real again. For neutron scattering this theory is formulated in terms of density matrices [23], and proposes that if the interaction time of the neutron with the target is of similar order of magnitude as the decoherence time, a reduced differential cross section should be observed in neutron scattering. Similar considerations would apply to electron scattering. Thus if the momentum transfer is high enough the scattering time will become comparable to the decoherence time, and the measurement should probe the proton wave function in the entangled proton-electron system.

In the impulse approximation the transfer of momentum to the proton does not affect the electronic structure. The bond may break, leading to electronic excitations, but this happens on a slower time-scale than the collision itself. Note that the bond strength of a C-H bond is $\simeq 4.5$ eV, larger than the energy transfer in the case of CH_4, but smaller than the energy transfer in the high-energy PE experiment. For the correlated electron-proton system the usual assumption that momentum can be transferred to the proton, without a probability of direct electronic excitations, could turn out to be wrong. This could transfer intensity from the proton peak to the background and hence be the cause of the missing proton intensity.

Electron-electron correlation gives rise to satellites in (e,2e) measurements, reducing the intensity of the main peak (see e.g. McCarthy *et al* [24]). Electron-proton correlation could have similar effects on the strength of the proton-derived elastic scattering peak.

4. Conclusions and Outlook

We measured the energy distribution of electrons scattered quasi-elastically from hydrocarbons both in the form of films and in the gas-phase. These experiments reveal information on the momentum distribution of the protons. There are currently problems reconciling the signal strength of the proton derived signal compared to the carbon derived signal for the solid films. Similar problems are present in neutron scattering experiments operating at comparable momentum transfer. Although there is currently not a full-fledged theory making quantitative predictions it is suggested that these discrepancies could be due to the quantum nature of the protons, probed at the short time scale of the collisions.

Especially the gas-phase measurement could provide a fertile testing ground of theory. Here there are no problems with energy-dependent backgrounds and/or radiation damage. Also neutron scattering can not as easily measure these low-density targets. Extending these measurements over a larger energy range could test the underlying theory (partial wave analysis, polarisation effects, impulse approximation and the possible quantum effects) in a way not easily accomplished by other means. The possibility of transferring kinetic energy to a single atom within a molecule is a fascinating one, especially if this energy is of the order of the chemical bond strength. Unfortunately the cross sections seem to be too small to detect molecular fragments in coincidence with the energy loss spectra, which would make the study of the break-up of molecules under these conditions possible.

References

[1] H. Boersch, R. Wolter, and H. Schoenebeck, Z. Physik **199**, 124 (1967).

[2] G. I. Watson, J. Phys.: Condens. Matter **8**, 5955 (1996).

[3] L. V. Hove, Phys. Rev. **95**, 249 (1954).

[4] V. F. Sears, Phys. Rev. B **30**, 44 (1984).

[5] M. Vos, G. P. Cornish, and E. Weigold, Rev. Sci. Instrum. **71**, 3831 (2000).

[6] B. Cranfill, Rev. Sci. Instrum. **49**, 264 (1978).

[7] Y. K. Godovsky and S. N. Magonov, Langmuir **16**, 3549 (2000).

[8] M. Vos, Phys. Rev A **65**, 12703 (2002).

[9] M. P. Paoli and R. S. Holt, J. Phys. C: Solid State Phys. **21**, 3633 (1988).

[10] J. C. Corchado and D. G. Truhlar, J. phys. Chem. A **102**, 1895 (1998).

[11] J. Mayers, T. M. Burke, and R. J. Newport, J. Phys.: Condens. Matter **6**, 641 (1994).

[12] A. Hitchcock, J. Electron Spectrosc. Relat. Phenom. **112**, 9 (2000).

[13] F. Salvat and R. Mayol, Comp. Phys. Commun. **74**, 358 (1993).

[14] M. Fink and J. Kessler, Z. Physik **196**, 1 (1966).

[15] M. Fink and R. A. Bonham, Phys. Rev. **187**, 114 (1969).

[16] M. Vos, C. Chatzidimitriou-Dreismann, T. Abdul-Redah, and J. Mayers, Nucl. Instr. and Meth. B **227**, 233 (2005).

[17] R. M. Brugger, A. D. Taylor, C. E. Olsen, J. A. Goldstone, and A. K. Soper, Nucl. Instrum. and Meth. **221**, 393 (1984).

[18] S. Lovesey, *Theory of Neutron Scattering from Condensed Matter* (Clarendon Press, Oxford, 1984), Vol. 1.

[19] C. A. Chatzidimitriou-Dreismann, T. Abdul-Redah, R. M. F. Streffer, and J. Mayers, Phys. Rev. Lett. **79**, 2839 (1997).

[20] C. A. Chatzidimitriou-Dreismann, T. Abdul-Redah, and R. M. Streffer, J. Chem. Phys. **116**, 1511 (2002).

[21] E. B. Karlsson, T. Abdul-Redah, R. M. F. Streffer, B. Hjörvarsson, J. Mayers, and C. A. Chatzidimitriou-Dreismann, Phys. Rev. B **67**, 184108 (2003).

[22] C. A. Chatzidimitriou-Dreismann, M. Vos, C. Kleiner, and T. Abdul-Redah, Phys. Rev. Lett. **91**, 57403 (2003).

[23] C. A. Chatzidimitriou-Dreismann, J. Alloys Comp. **356-357**, 244 (2003).

[24] I. E. McCarthy, R. Pascual, P. Storer, and E. Weigold, Phys. Rev. A **40**, 3041 (1989).